ORGANOMETALLICS

Article

pubs.acs.org/Organometallics

Synthesis and Reactivity of a Terminal Scandium Imido Complex

Terry Chu, Warren E. Piers,* Jason L. Dutton,† and Masood Parvez

Department of Chemistry, University of Calgary, 2500 University Drive NW, Calgary, Alberta, Canada T2N 1N4

Supporting Information

ABSTRACT: Preparation of a terminal scandium imido complex, **2**·DMAP, was accomplished through thermolysis of an arylamido methyl complex, **1**, stabilized by a bulky β-diketiminato ligand in the presence of 4-*N*,*N*-dimethylaminopyridine (DMAP). Mechanistic studies revealed that the reaction proceeds by initial metalation of **1**, followed by rapid DMAP-promoted alkane elimination to generate the scandium imido complex. Kinetic studies of the reaction between separately synthesized metalate **3** and DMAP under pseudo-first-order conditions yielded activation parameters of $\Delta H^{\ddagger}$ = 73.5(2) kJ mol^{-1} and $\Delta S^{\ddagger}$ = −70.4(5) J K^{-1} mol^{-1}. The reaction of **2**·DMAP with *tert*-butyl amine or phenylacetylene resulted in addition of the N−H or C−H bond across the scandium imide linkage, respectively, to furnish complexes *endo*-/*exo*-**4** and *endo*-**5**. These compounds were fully characterized, including via structural analysis, providing further evidence for the terminal scandium imido derivative **2**·DMAP.

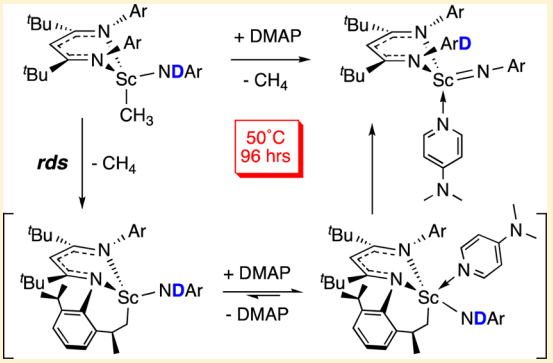

INTRODUCTION

Terminal imido ligands play a central role in various aspects of early-transition-metal chemistry. As potential 2σ−4π, six-electron donors,[1] they are isolobal with the ubiquitous cyclopentadienide anion and have been used as a Cp substitute in an ancillary role in the organometallic chemistry of metals from groups 4,[2−4] 5, and 6.[5−7] On the other hand, in part because of the variable bond order possible in the M═N bond, they can be highly reactive ligands and serve as intermediates in important catalytic reactions such as imine metathesis[8] and early-transition-metal-catalyzed hydroamination cycles.[9−13] Furthermore, as discovered in seminal papers by Bergman[14] and Wolczanski,[15] terminal early-metal imides can activate the C−H bonds of hydrocarbons, including methane.[16−18] Thus, the terminal imido ligand is a versatile chemical entity in the chemistry of the group 4−6 metals.

Less is known about their role in group 3 metal or lanthanide chemistry.[19] Indeed, several groups have attempted to prepare terminal imido compounds of these more electropositive metals and map out their chemistry, but while inroads have been made, such compounds remain rare and elusive. One issue is the prevention of dimerization through use of a ligand environment of suitable bulk. For example, although Hessen et al. postulated the intermediacy of a terminal imido scandium species supported by a cyclopentadienyl amino ligand,[20] the compound was isolated and characterized as a dimer. This issue is exacerbated in larger group 3 metals and lanthanides.[21−24] A second factor concerns the potentially high reactivity of the Ln═NR bond, documented by Mindiola and co-workers in a P−N−P pincer ligand supported scandium complex.[25] Here, convincing evidence for the intermediacy of a terminal scandium imido derivative was presented, but the addition of an α-C−H bond of coordinated pyridine could not be prevented, and so an amido complex was the isolated product.

Our own attempts to generate β-diketiminato ("nacnac") supported terminal imido scandium complexes using high-temperature-induced alkane elimination methodologies (pioneered by Bergman[14] and Wolczanski[15] for the group 4 metal systems) with the scandium nacnac amido alkyl derivative **I** met with failure.[26] Very recently, however, the group of Chen solved this problem by incorporating a pendant amine donor into the nacnac ligand framework and induced alkane elimination by use of an external 4-*N*,*N*-dimethylaminopyridine (DMAP) donor. They thus were able to report the first crystallographically characterized terminal scandium imido complex, the five-coordinate derivative **II**.[27] Subsequent papers from this group disclosed a second five-coordinate derivative (**III**) and reported on the reactivity of these novel species.[28,29] Essentially, the use

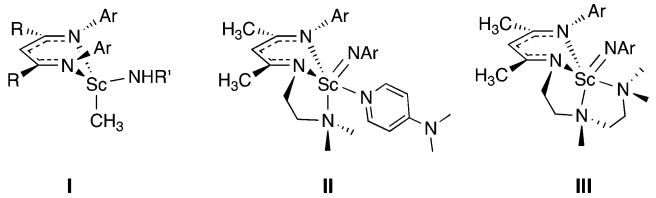

I II III

of internal or external donors was key to inducing alkane elimination from the amido alkyl precursors at low enough temperatures that the product imido complex was thermally stable. The downside of this approach is that the resulting

Special Issue: Recent Advances in Organo-f-Element Chemistry

Received: September 26, 2012
Published: November 2, 2012

dx.doi.org/10.1021/om300913d | *Organometallics* 2013, 32, 1159−1165

terminal imido complexes are more coordinatively saturated and therefore less reactive. We thus thought to revisit our earlier chemistry involving nacnac derivatives of **I** by adopting the Chen strategy of using an external base to induce alkane elimination, as opposed to thermolysis, and generate lower coordinate scandium terminal imido derivatives; these results are described herein.

RESULTS AND DISCUSSION

The arylamido alkyl nacnac complex **1** (Scheme 1) was reported by us in 2004 as a potential precursor to a scandium

Scheme 1

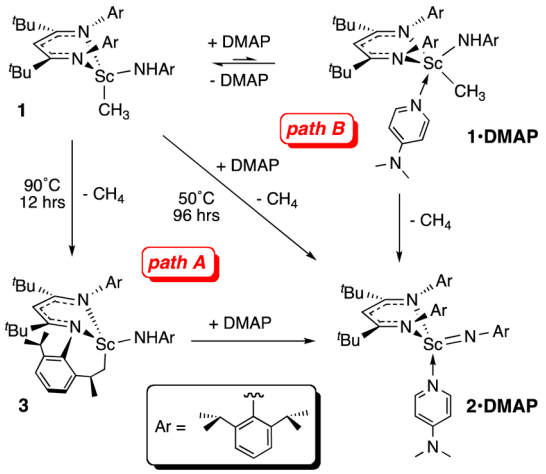

imido complex via thermally induced methane elimination.[26] Although methane elimination was observed upon heating solutions of the complex to 90 °C, the observed product was the metalated species **3**, which was fully characterized (vide infra). Furthermore, deuterium labeling experiments showed that metalates closely related to **3** are formed directly, without the intermediacy of the anticipated imido species.[26,30]

In contrast, when **1** was heated at 50 °C in the presence of DMAP, no evidence for metalation product **3** was observed in the ^{1}H NMR spectrum. Rather, smooth conversion over the course of 4−5 days to a different product, assigned as the DMAP-stabilized terminal imido complex **2**·DMAP, was observed. During the reaction, the resonance at 0.03 ppm for the Sc-Me group in **1** gradually disappeared and that for CH_4 grew in (Figure 1), concurrent with the appearance of signals for **2**·DMAP. Instead of the complex set of ligand resonances characteristic of the highly unsymmetrical metalated derivative **3**,[26,31] **2**·DMAP exhibited nacnac ligand resonance patterns seen in C_s-symmetric derivatives with two different ligands bonded to the (nacnac)Sc fragment.[31,32] Thus, one singlet for the ^{t}Bu protons was accompanied by four doublets and two septets for the β-diketiminato N-aryl isopropyl methyl and methine protons, respectively. Upfield-shifted resonances at 6.37, 5.77, and 2.14 ppm for the coordinated DMAP ligand were distinct from those observed for free DMAP (cf. 8.36, 6.08, and 2.29 ppm). The backbone CH proton is observed at 5.92 ppm, while the characteristic NH resonance for the arylamido ligand in **1** was absent from the spectrum. Finally, two doublets and two septets were observed for the isopropyl groups of the imido N-aryl substituent, suggesting that this ring is oriented in the plane of symmetry of the molecule as depicted in Scheme 1 and that there is restricted rotation about

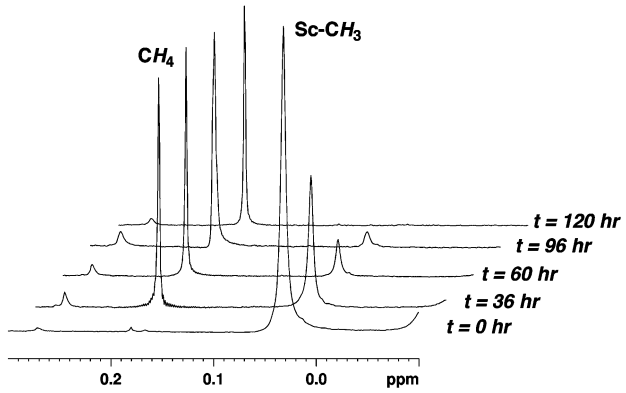

Figure 1. Partial 400 MHz ^{1}H NMR spectrum of a mixture of **1** and DMAP heated at 50 °C in C_6D_6 showing the loss of the Sc−CH_3 resonance and the appearance of CH_4.

the N_{imido}−C_{aryl} bond, rendering the isopropyl groups diastereotopic. Although numerous attempts were made to grow crystals of **2**·DMAP, samples suitable for X-ray analysis eluded us. Nevertheless, elemental analysis data are consistent with this formulation and reactivity studies of this compound as described below confirm its identity as assigned.

The mechanism by which **2**·DMAP is formed from **1** can occur by two plausible pathways, paths A and B, as shown in Scheme 1. In path A, metalation occurs first, followed by (relatively) rapid, DMAP-prompted alkane elimination from **3**. In path B, DMAP coordinates to **1**, inducing methane elimination to give the imido derivative **2**·DMAP. Several lines of experimental evidence indicate that the former path (path A) is operative. First, heating is required for this reaction to proceed, the optimal temperature being 50 °C to prevent product degradation. Higher temperatures would presumably favor the left-hand side of the equilibrium at the top of Scheme 1 but would promote metalation to produce **3**. Second, when **1** is mixed with DMAP, even at low temperature, no evidence for formation of the adduct **1**·DMAP is apparent in the ^{1}H NMR spectrum; only signals for **1** and free DMAP are observed. Thus, the equilibrium constant is very small ($<10^{-2}$ L mol^{-1}) for this complexation. Third, and most telling, when *d*-**1** (selectively labeled at the arylamido position) was heated in the presence of DMAP, only CH_4 was observed (i.e., no CH_3D was produced), and in the ^{2}H NMR spectrum, signals at 0.74 and 1.30 ppm coinciding with two of the methyl resonances in the isopropyl substituents on the N-aryl groups of **2**·DMAP were observed. These observations are completely consistent with rate-limiting metalation and elimination of methane followed by rapid reaction between **3** and DMAP to give **2**·DMAP.

This postulate suggests that separately synthesized **3** should react rapidly with DMAP to furnish the product **2**·DMAP. Accordingly, metalate **3** was synthesized on a preparative scale by thermolysis of **1** in the absence of DMAP. It was isolated as a yellow solid in 53% after workup and exhibited a characteristic pattern of resonances in the ^{1}H NMR spectrum for this desymmetrized structure.[26] A resonance at 4.17 ppm for the retained N*H* proton and an AB quartet centered at 0.48 ppm for the diastereotopic ScCH_2 protons of the metalated isopropyl methylene group are particularly diagnostic. An X-ray analysis on crystals obtained from a concentrated hexanes solution was not of high enough quality to obtain metrical data of meaningful accuracy but certainly established the connectivity within the molecule (Figure S1, Supporting

dx.doi.org/10.1021/om300913d | *Organometallics* 2013, 32, 1159−1165

Scheme 2

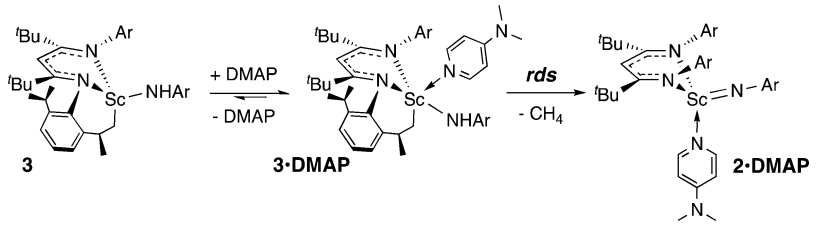

Information), which is similar to that found for a previously characterized derivative in which the group on the amido nitrogen is ^{t}Bu rather than the 2,6-diisopropylphenyl group in **3**.[26,33] Reaction of isolated, pure metalate **3** with 1 equiv of DMAP results in a rapid color change from yellow to red followed by gradual lightening of the solution over the course of a few hours at room temperature. Monitoring the reaction by ^{1}H NMR spectroscopy shows that the red color is likely due to a DMAP adduct of **3**; signals for free DMAP and **3** are supplanted by those for coordinated DMAP and a second unsymmetrical species (**3**·DMAP). Loss of CH_4 is accompanied by the growing in of signals for **2**·DMAP. Thus, it appears that rapid DMAP coordination is followed by rate-limiting loss of methane to give the imido product (Scheme 2).

Kinetic studies are completely consistent with this postulate. When **3** is reacted with 10, 15, 20, and 25 equiv of DMAP (pseudo-first-order conditions) at 295 K, while there is a steady increase in the observed pseudo-first-order rate constant, the effect is slight and not indicative of first-order behavior in [DMAP] (Figure 2a). Instead, this effect is likely reflective of

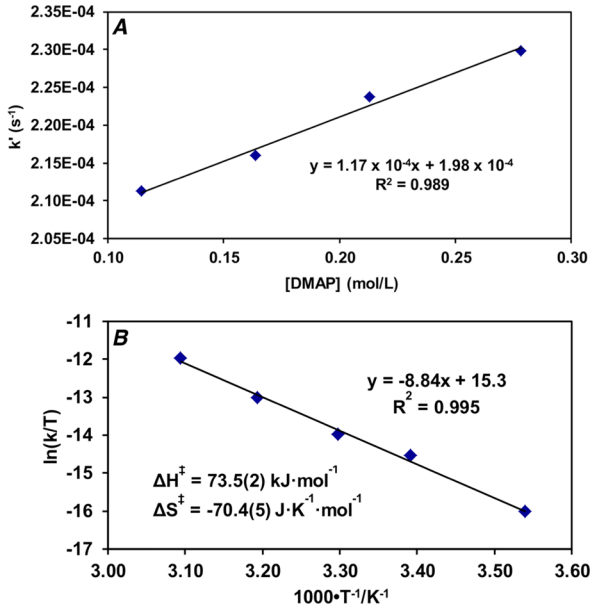

Figure 2. (A) Plot of the observed pseudo-first-order rate constant for the formation of **2**·DMAP as a function of [DMAP]. (B) Eyring plot for the formation of **2**·DMAP (15 equiv of added DMAP).

the shifting of the adduct-forming equilibrium toward **3**·DMAP as the DMAP concentration is increased. An Eyring plot obtained by measuring the pseudo-first-order rate constant for the reaction of **3** with 15 equiv of DMAP at various temperatures ranging from 282 to 323 K gives activation parameters of $\Delta H^{\ddagger}$ = 73.5(2) kJ mol^{-1} (17.6 kcal mol^{-1}) and $\Delta S^{\ddagger}$ = −70.4(5) J K^{-1} mol^{-1} (−16.8 cal K^{-1} mol^{-1}) (Figure 2b). This is a somewhat smaller enthalpic barrier than that recorded for alkane elimination in a comparable zirconium system (25.9 kcal mol^{-1})[15] but a higher entropic barrier; the value of $\Delta S^{\ddagger}$ in the Zr system was −7 eu. Here, the role of the external base DMAP serves to lower the enthalpic barrier but may require extra ordering in the transition state as a result.

The necessary intermediacy of **3** to increase the facility of alkane elimination to yield a scandium imido group is interesting. Direct methane elimination from **1** appears to be precluded because the metal center is too hindered to allow for coordination of DMAP but not crowded enough to stimulate methane elimination across the Sc−N bond. Loss of methane via metalation to produce **3** creates more open space about the metal, allowing for DMAP coordination but also perhaps provides strain release energy as a driving force for the subsequent alkane elimination step leading to Sc═N bond formation. Other examples where a premetalation step aids in overcoming energetically difficult steps[34,35] or leads to facile metalate ring opening[36] have appeared in the literature.

Our inability to obtain X-ray structural data on **2**·DMAP raises a kernel of doubt concerning its assignment as a monomeric scandium terminal imide. While the observation of only one signal in the ^{1}H NMR spectrum for the nacnac ligand backbone suggests that dimers are not present,[37] it is possible that only one of the three possible dimeric isomers is energetically feasible.[38] Unfortunately, mass spectroscopic analysis was precluded by the high air and water sensitivity of the compound and IR spectroscopy was inconclusive; therefore, we explored derivatization reactions as a means for providing further evidence for our structural assignment of **2**·DMAP.

No reaction of **2**·DMAP with *tert*-butylamine or phenylacetylene was observed at room temperature, but upon heating to 70 °C in the presence of these reagents, clean conversion to new products was observed to occur over the course of 72 h (Scheme 3). These products were identified as the diastereoisomers of the mixed bis-amido complex **4** (the endo and exo designations here refer to the position of the newly introduced *tert*-butylamido group) and the phenylacetylido arylamido complex *endo*-**5** (the endo designation here refers to the acetylido group). The identity of these products was confirmed through their separate synthesis from a suitable amido chloride precursor[26] and either LiNHAr or LiCCPh, as shown in the bottom right corner of Scheme 3. The products arise from addition of an N−H bond in ^{t}BuNH$_2$ or the acetylenic C−H bond in PhCCH across the Sc═N bond in **2**·DMAP; as for **1**, these products do not coordinate the free DMAP that is released in this reaction, which is washed away in workup. Consistent with this proposal, use of deuterated reagents (^{t}BuND$_2$ or PhCCD) resulted in d_2-*endo*-/*exo*-**4** or *d*-*endo*-**5**, respectively, labeled exclusively at the amido N*D* positions. In the case of **4**, the two C_s-symmetric isomers, present in a 2:1 equilibrium ratio, are in slow exchange on the ^{1}H NMR time

dx.doi.org/10.1021/om300913d | *Organometallics* 2013, 32, 1159−1165

Scheme 3

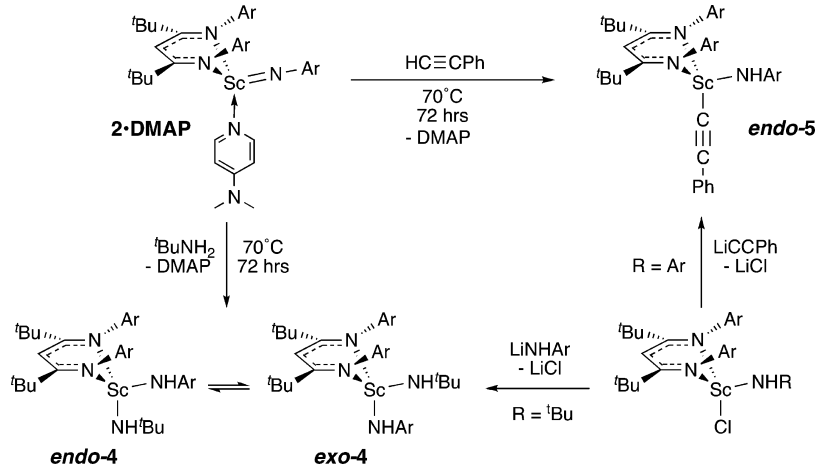

scale; therefore, the spectrum is complex. We were unable to conclusively assess which isomer was the major one and which was the minor. Typically, for electronically similar ligands, the sterically more bulky ligand is favored in the exo position;[31] the isomer *endo*-**4** was that present in the single crystal that was analyzed by X-ray diffraction (vide infra), but this does not necessarily mean that this is the major isomer in solution. In the case of *endo*-**5**, only one isomer is observed in solution. Since we have shown that stronger π donors are also favored in the exo position,[26] it is likely this isomer is the one with the acetylide ligand in the endo position; this was confirmed by X-ray diffraction. The exclusive observation of C−H activation in the reaction with phenylacetylene is interesting, since metallacycle formation via 2 + 2 addition is also a possible reaction channel.[39]

Figure 3 shows the molecular structure of *endo*-**4**, along with selected metrical data, and Figure 4 does the same for *endo*-**5**.

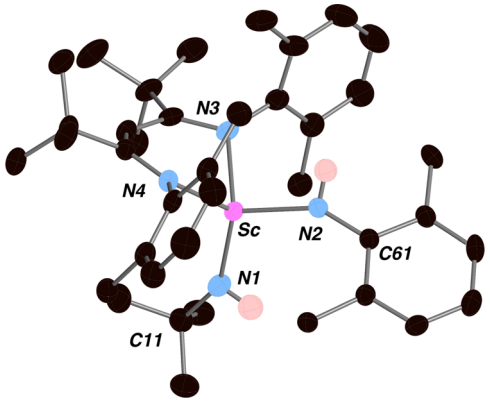

Figure 3. Thermal ellipsoid diagram (50% probability) of *endo*-**4**. Isopropyl methyl groups on the Ar substituents have been removed for clarity. Selected bond distances (Å): Sc−N(1), 2.005(2); Sc−N(2), 2.040(2); Sc−N(3), 2.126(2); Sc−N(4), 2.196(2). Selected bond angles (deg): N(1)−Sc−N(2), 110.88(9); N(3)−Sc−-N(4), 91.04(8); Sc−N(1)−C(11), 149.26(18); Sc−N(2)−C(61), 146.84(17).

As in the several other structures for compounds in this family, the scandium centers lie out of the plane defined by the C_3N_2 ligand atoms; the metrical data for the nacnac ligand framework are similar to those found in other complexes and analyzed in detail elsewhere.[31] The other ligands bound to these four-coordinate scandium centers also exhibit standard character-

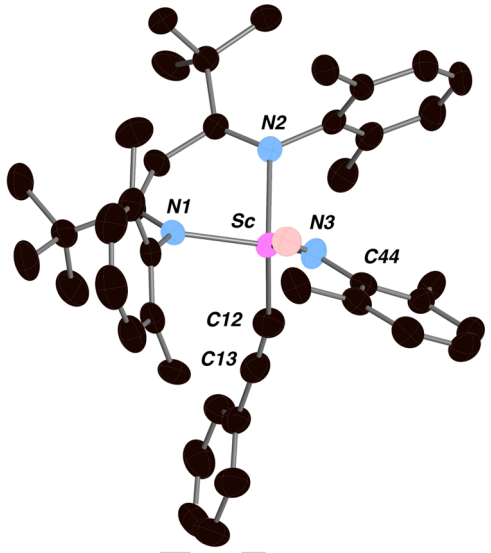

Figure 4. Thermal ellipsoid diagram (50% probability) of *endo*-**5**. Isopropyl methyl groups on the Ar substituents have been removed for clarity. Selected bond distances (Å): Sc−N(1), 2.072(2); Sc−N(2), 2.163(2); Sc−N(3), 2.023(3); Sc−C(12), 2.194(3). Selected bond angles (deg): N(1)-Sc−N(2), 91.05(9); N(3)−Sc−C(12), 122.14(12); Sc−N(3)−C(44), 145.7(2); Sc−C(12)−C(13), 165.6(3).

istics; the primary amido ligands have short Sc−N distances ranging from 2.004(2) to 2.039(2) Å, consistent with strong π bonding from nitrogen to scandium. Consequently, the Sc−N_{amido}−C bond angles are rather large, ranging from 145.7(2) to 149.17(16)°. In *endo*-**5**, the Sc−C(12) bond length of 2.194(3) Å is slightly shorter than the typical distance of ∼2.22 Å for Sc−C(sp^3) bonds, as might be expected due to the sp hybridization at C(12). The Sc−$C_{acetylide}$ distances in a six-coordinate complex with two phenylacetylide ligands are 2.262(3) and 2.296(4) Å.[40]

The full characterization of these two products strongly suggests that **2**·DMAP is a terminal imido species in which the DMAP ligand stabilizes a highly reactive three-coordinate imido complex: i.e., **2** (Scheme 4). Despite the fact that *tert*-butylamine and phenylacetylene are chemically very different reagents, the rates of their reaction with **2**·DMAP are (qualitatively at least) very similar, occurring slowly at 70 °C over the course of a few days. This observation suggests that

dx.doi.org/10.1021/om300913d | *Organometallics* 2013, 32, 1159−1165

Scheme 4

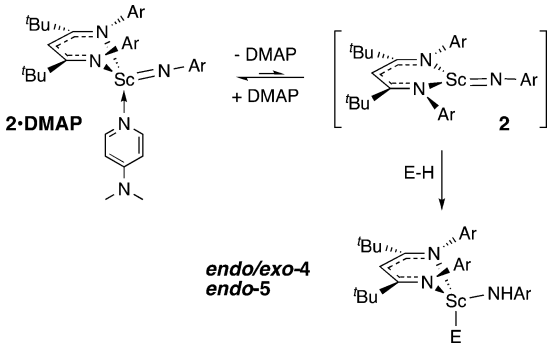

these reactions proceed via rate-limiting dissociation of DMAP to produce a highly reactive scandium imide that rapidly adds the E−H bond of the reagent to form the products (Scheme 4). Attempts to observe exchange between free and coordinated DMAP by high-temperature ^{1}H NMR spectroscopy or EXSY spectroscopy experiments were not successful, suggesting that this process is slow on the NMR time scale. Thus, although quantitative kinetic experiments have not been performed, it is likely that dissociation of DMAP from **2**·DMAP is required in order for these reactions to proceed.

In summary, we have utilized the Lewis base promoted alkane elimination reaction to access a four-coordinate scandium imide. Mechanistic studies show that the formation of **2**·DMAP proceeds indirectly via a metalated product rather than directly from the methyl arylamido starting material. Although not structurally characterized, spectroscopic data and its reactivity toward an N−H bond in *tert*-butylamine and the acetylenic C−H bond of phenylacetylene are strong evidence for the assignment of **2**·DMAP as a terminal imido derivative.

EXPERIMENTAL SECTION

General Procedures and Equipment. An argon atmosphere MBraun glovebox was employed for manipulation and storage of all oxygen and moisture-sensitive compounds. Reactions were performed on a double-manifold high-vacuum line using standard techniques. Toluene and hexane were dried and purified using the Grubbs/Dow purification system[41] and stored in evacuated glass vessels over sodium/benzophenone ketyl. Pentane was predried and distilled from 3 Å molecular sieves and then stored over sodium/benzophenone in evacuated glass vessels. d_6-Benzene and d_8-toluene were predried and distilled from sodium/benzophenone and stored in a glass vessel in the glovebox. NMR spectra were obtained on Bruker DRX400, AVANCE 400 MHz, and AVANCE III 400 MHz spectrometers. ^{1}H and ^{13}C{^{1}H} chemical shifts were referenced to residual proton and naturally abundant ^{13}C resonances of the deuterated solvent, respectively, relative to tetramethylsilane. NMR spectra were processed and analyzed with MestReNova software (v6.2.1−7569). 4-*N*,*N*-dimethylaminopyridine (DMAP), 2,6-di-*iso*-propylaniline (NH_2Dipp), *tert*-butylamine ($NH_2{}^t$Bu), and phenylacetylene were purchased from Aldrich Chemicals and purified using standard methods. Amines and phenylacetylene were predried and distilled from 3 Å molecular sieves and then stored over fresh sieves in the glovebox. Lithium amides were prepared by lithiation with 1 equiv of ^{n}BuLi to produce LiNHR (R = Dipp, ^{t}Bu) salts.[42] Lithium phenylacetylide was isolated from the reaction of phenylacetylene and 1 equiv of ^{n}BuLi.[43] For the deuterium labeling studies, D_2NDipp and D_2N^tBu were prepared according to the literature procedure.[44] Quenching lithium phenylacetylide with excess D_2O followed by distillation under an argon atmosphere allowed for the preparation of *d*-phenylacetylene.[35] Compounds $LScCl_2$ (**A**),[31] LScClNHAr (**B**),[26] $LScMe_2$ (**C**),[31] and LScClNH^{t}Bu (**D**)[26] were prepared according to literature procedures. Elemental analyses were obtained by the Instrumentation Facility of the Department of Chemistry. Details on the X-ray analyses can be found in the deposited CIF files (Supporting Information) or via the Cambridge Crystallographic Data Centre (CCDC 902751 and 902752).

Synthesis of 1. Compound **1** was prepared by a modified literature procedure.[26] A 50 mL flask was charged with **A** (0.500 g, 0.809 mmol) and methyllithium (0.071, 3.230 mmol). Toluene (25 mL) was condensed into the evacuated flask at −78 °C. The mixture was warmed to room temperature and stirred for 2 h. The reaction mixture was filtered, and NH_2Dipp (0.150 mL, 0.809 mmol) was added via syringe and then stirred at room temperature for 12 h. The toluene was removed in vacuo to afford an orange solid. Hexanes (25 mL) was condensed into the flask and the assemblage sonicated for 20 min; the hexanes was then removed to give a yellow solid (0.490 g, 0.664 mmol, 82%). The spectroscopic data are consistent with previously published data.[26]

Generation of 1-*d*. An NMR tube was charged with **C** (0.015 g, 0.026 mmol) and D_2NDipp (5.00 μL, 0.026 mmol) in 0.6 mL of d_8-toluene. The tube was shaken and left at room temperature for 12 h. The ^{1}H NMR spectrum matched that of **1**, except that no resonance was observed for the amido proton. ^{2}H NMR (C_7D_8): δ 5.44 (s, N*D*).

Synthesis of 2·DMAP. *Method A.* **1** (0.150 g, 0.203 mmol) and DMAP (0.025 g, 0.203 mmol) were charged in a 50 mL flask dissolved in 10 mL of toluene. The solution was heated to 50 °C under argon for 5 days. After the heating was completed, toluene was removed in vacuo and hexanes (10 mL) was condensed into the flask and sonicated for 20 min. Evaporation of hexanes yielded 0.109 g of a fluffy yellow powder (0.129 mmol, 64%).

Method B. Toluene (15 mL) was condensed into an evacuated flask containing **1** (0.200 g, 0.271 mmol) at −78 °C. The mixture was heated with stirring at 90 °C for 12 h. In a separate vial, DMAP (0.035 g, 0.271 mmol) was dissolved in toluene (5 mL) and added to the flask via syringe. The reaction mixture was stirred for 12 h at room temperature. Solvent was removed to yield an orange oil, and hexanes (10 mL) was condensed into the flask and sonicated for 20 min. Removal of the solvent in vacuo afforded 0.158 g of a fine yellow powder (0.187 mmol, 69%). ^{1}H NMR (C_7D_8): δ 7.20−6.96 and 6.78 (m, 9H, Ar*H*), 6.65 (d, 2H, *o-H* py-NMe_2, $^3J_{H-H}$ = 6.2 Hz), 5.92 (s, 1H, C*H*), 5.76 (dd, 2H, *m-H* py-NMe_2, $^3J_{H-H}$ = 6.2 Hz), 3.82 (sp, 2H, C*H*Me_2, $^3J_{H-H}$ = 6.8), 3.44 (sp, 1H, NH-2,6-(C*H*Me_2)$_2C_6H_3$, $^3J_{H-H}$ = 6.8 Hz), 3.11 (sp, 1H, NH-2,6-(C*H*Me_2)$_2C_6H_3$, $^3J_{H-H}$ = 6.8 Hz), 2.89 (sp, 2H, C*H*Me_2, $^3J_{H-H}$ = 6.8 Hz), 2.14 (br s, 6H, py-NMe_2), 1.4, (ov d, 12H, CHMe_2 and NH-2,6-(CHMe_2)$_2C_6H_3$), 1.30 (d, 6H, CHMe_2, $^3J_{H-H}$ = 6.8 Hz), 1.27 (br s, 18H, NCCMe_3), 1.23 (d, 6H, CHMe_2, $^3J_{H-H}$ = 6.8 Hz), 0.90 (d, 6H, NH-2,6-(CHMe_2)$_2C_6H_3$, $^3J_{H-H}$ = 6.8 Hz), 0.74 (d, 6H, CHMe_2, $^3J_{H-H}$ = 6.8 Hz). ^{13}C{^{1}H} NMR (C_7D_8): δ 175.6 (N*C*Me_3), 153.0 (*p-C* py-NMe_2), 151.8, 146.8, 144.0, 142.7, 142.1, 137.3, 132.0, 124.4, 124.2, 123.8, 122.4, and 116.7 (Ar*C*) 110.0 (*o-C* py-NMe_2), 107.5 (*m-C* py-NMe_2), 95.3 (*C*H), 44.9 (N*C*Me_3), 38.72 (py-NMe_2), 33.5 (NC*C*Me_3), 29.9 and 28.9 (CHMe_2), 29.3 and 28.9 (NH-2,6-(CHMe_2)$_2C_6H_3$), 27.6, 25.8, 24.8, and 24.7 (CHMe_2), 25.8 and 25.1 (NH-2,6-(CHMe_2)$_2C_6H_3$). Anal. Calcd for $C_{54}H_{80}N_5Sc$: C, 76.83; H, 9.55; N, 8.30. Found: C, 77.03; H, 9.88; N, 8.05.

Synthesis of 3. In an evacuated flask at −78 °C containing **1** (0.200 g, 0.271 mmol) toluene (10 mL) was condensed. The solution was heated at 90 °C for 12 h and solvent removed under vacuum, yielding an orange oil. Hexanes (10 mL) was added, and the mixture was sonicated for 15 min. The hexane was removed in vacuo, affording an orange powder. Hexamethyldisiloxane (7 mL) was transferred onto the powder and cooled to −30 °C for 1 h. The mixture was filtered and solvent removed to afford a yellow powder (0.102 g, 0.141 mmol, 53%). X-ray-quality crystals were grown from concentrated pentane solutions at −35 °C. ^{1}H NMR (C_7D_8): δ 7.25−6.80 and 6.66 (m, 9H, Ar*H*), 5.82 (s, 1H C*H*), 4.17 (br s, 1H, N*H*), 3.41 (sp, 1H, C*H*Me_2, $^3J_{H-H}$ = 6.8 Hz), 3.25 (m, 1H, CH_2C*H*Me), 3.13 (m, 2H, C*H*Me_2), 2.07 (sp, 2H, NH-2,6-(C*H*Me_2)$_2C_6H_3$, $^3J_{H-H}$ = 6.4 Hz), 1.47 (d, 3H, CHMe_2, $^3J_{H-H}$ = 6.7 Hz), 1.29−1.22 (m, 15H, CHMe_2), 1.18 (d, 3H, CH_2CH*Me*, $^3J_{H-H}$ = 6.8 Hz), 1.11 (br s, 9H, NCCMe_3), 1.08 (m, 10H, NCCMe_3 and CH_2CHMe), 0.90 (d, 12H, NH-2,6-(CHMe_2)$_2C_6H_3$, $^3J_{H-H}$ = 6.6 Hz) and 0.48 (ov dd, 1H, CH_2CHMe). ^{13}C{^{1}H} NMR

dx.doi.org/10.1021/om300913d | *Organometallics* 2013, 32, 1159−1165

(C_7D_8): δ 175.9 and 175.5 ($NCCMe_2$), 149.9, 148.9, 144.6, 142.9, 142.0, 141.5, 133.8, 126.9, 124.2, 122.8, 122.6, 117.0 (ArC), 99.7 (CH), 55.3 ($ScCH_2$), 43.7 and 42.8 ($NCCMe_3$), 38.9 (CH_2CHCH_3), 32.8 and 31.6 ($NCCMe_3$), 29.7 (NH-2,6-$(CHMe_2)_2C_6H_3$), 28.8, 28.6, and 28.5 ($CHMe_2$), 26.0, 25.2, 25.1, 25.0, 24.5, 23.2, 22.1 ($CH(CH_3)_2$), 24.7 (NH-2,6-$(CHMe_2)_2C_6H_3$). Anal. Calcd for $C_{47}H_{70}N_3Sc$: C, 78.18; H, 9.77; N, 5.82. Found: C, 78.34; H, 9.85; N, 6.04.

Generation of *d*-3. *d*-**1** (0.019 g, 0.026 mmol) was dissolved in 0.6 mL of d_8-toluene. The solution was mixed thoroughly and heated to 90 °C for 12 h. The ^{1}H NMR spectrum matched that of **3**, except that no resonances were observed for the amido proton. ^{2}H NMR (C_7D_8): δ 4.30 (br s, N*D*).

Synthesis of *endo*-/*exo*-4. *Method A.* An NMR tube was charged with **2**·DMAP (0.008 g, 9.483×10^{-3} mmol) and $NH_2{}^tBu$ (1.00 μL, 9.483×10^{-3} mmol) in 0.6 mL of d_8-toluene. The tube was shaken and heated at 70 °C for 3 days.

Method B. A 50 mL flask was charged with **D** (0.215 g, 0.329 mmol) and solid LiNHDipp (0.066 g, 0.361 mmol). Toluene (25 mL) was condensed into the evacuated flask at −78 °C. The mixture was heated to 70 °C and stirred for 12 h. The toluene was removed in vacuo to afford an orange solid. Hexanes (25 mL) was condensed into the flask and the assemblage sonicated for 20 min. The reaction mixture was filtered and hexanes removed to afford a yellow solid (0.243 g, 0.306 mmol, 93%). X-ray-quality crystals were grown from a concentrated hexanes solution at room temperature. ^{1}H NMR for the major isomer (C_7D_8): δ 7.12−6.84 and 6.64 (m, 9H, Ar*H*), 5.83 (s, 1H, C*H*), 5.29 (s, 1H, N*H*-2,6-$(CHMe_2)_2C_6H_3$), 3.89 (sp, 2H, $CHMe_2$, $^3J_{H-H}$ = 6.7 Hz), 3.06 (ov sp, 2H, $CHMe_2$, $^3J_{H-H}$ = 6.8 Hz), 3.40 (s, 1H, N*H*-^{t}Bu), 2.16 (sp, 2H, NH-2,6-$(CHMe_2)_2C_6H_3$, $^3J_{H-H}$ = 6.4 Hz), 1.42 (d, 6H, $CHMe_2$, $^3J_{H-H}$ = 6.7 Hz), 1.36 (d, 6H, $CHMe_2$, $^3J_{H-H}$ = 6.6 Hz), 1.21 (d, 6H, $CHMe_2$, $^3J_{H-H}$ = 6.7 Hz), 1.17 (s, 9H, NH-^{t}*Bu*), 1.14 (s, 18H, $NCCMe_3$), 1.10 (d, 6H, $CHMe_2$, $^3J_{H-H}$ = 6.7 Hz), 0.92 (d, 12H, NH-2,6-$(CHMe_2)_2C_6H_3$, $^3J_{H-H}$ = 6.6 Hz). Complete assignment of the ^{1}H NMR for the minor isomer was not possible, due to signal overlap with the other diastereomer. ^{1}H NMR for the minor isomer (C_7D_8): δ 7.12−6.84 and 6.64 (m, 9H, Ar*H*), 5.82 (s, 1H, C*H*), 5.04 (s, 1H, N*H*-2,6-$(CHMe_2)_2C_6H_3$), 4.15 (s, 1H, N*H*-^{t}Bu), 3.42 (ov sp, 2H, NH-2,6-$(CHMe_2)_2C_6H_3$, $^3J_{H-H}$ = 6.8 Hz), 3.06 (ov sp, 2H, $CHMe_2$, $^3J_{H-H}$ = 6.8 Hz), 1.30 (s, 18H, $NCCMe_3$), 1.27 (m, 12H, $CHMe_2$), 0.72 (s, 9H, NH-^{t}*Bu*). Complete assignment of the ^{13}C{^{1}H} NMR spectrum was not possible, and such data are reported by carbon type: δ 150.5, 149.5, 144.7, 144.1, 142.8, 142.7, 142.0, 141.0, 134.0, 126.4, 126.0, 125.2, 124.5, 124.4, 124.0, 123.0, 117.4, and 117.2 (ArC), 27.88, 26.29, 26.03, 24.99, 24.92, and 24.84 ($CHMe_2$). All other carbon resonances were attributable to a specific diastereomer. ^{13}C{^{1}H} NMR for exo_{NHtBu} (C_7D_8): δ 176.0 ($NCCMe_3$), 94.83 (CH), 54.48 ($NHCMe_3$), 44.56 ($NCCMe_3$), 35.01 ($NHCMe_3$), 32.64 ($NCCMe_3$), 29.22 (NH-2,6-$(CHMe_2)_2C_6H_3$), 28.46 and 27.15 ($CHMe_2$) 24.69 (NH-2,6-$(CHMe_2)_2C_6H_3$). ^{13}C{^{1}H} NMR for $endo_{NHtBu}$ (C_7D_8): δ 175.6 ($NCCMe_3$), 93.01 (CH), 53.88 ($NHCMe_3$), 44.68 ($NCCMe_3$), 34.07 ($NHCMe_3$), 32.87 ($NCCMe_3$), 29.77 (NH-2,6-$(CHMe_2)_2C_6H_3$), 28.25 and 26.69 ($CHMe_2$), 24.80 (NH-2,6-$(CHMe_2)_2C_6H_3$). Anal. Calcd for $C_{51}H_{81}N_4Sc$: C, 77.03; H, 10.27; N, 7.05. Found: C, 76.98; H, 10.26; N, 6.90.

Generation of d_2-*endo*-/*exo*-4. An NMR tube was charged with **2**·DMAP (0.015 g, 0.018 mmol) and D_2N^tBu (2.00 μL, 0.018 mmol) in 0.6 mL of d_8-toluene. The tube was shaken and heated at 70 °C for 3 days. The ^{1}H NMR spectrum matched that of *endo*-/*exo*-**4**, except that no resonances were observed for the amido protons. ^{2}H NMR (C_7D_8): δ 5.10 (br s, N*D*-2,6-$(CHMe_2)_2C_6H_3$), 1.08 (br s, N*D*-^{t}Bu).

Synthesis of *endo*-5. *Method A.* **2**·DMAP (0.007 g, 9.106×10^{-3} mmol) and phenylacetylene (1.00 μL, 9.106×10^{-3} mmol) were dissolved in 0.6 mL of d_8-toluene. The solution was mixed thoroughly and heated to 70 °C for 72 h.

Method B. Toluene (20 mL) was condensed into an evacuated flask containing **B** (0.150 g, 0.198 mmol) and lithium phenylacetylide (0.024 g, 0.218 mmol) at −78 °C. The solution was stirred at 80 °C for 12 h, upon which the solvent was removed under vacuum. The orange oil was sonicated in hexanes (20 mL) for 20 min and then filtered to afford a yellow solution. Removal of the solvent in vacuo afforded a tacky orange solid. Crystals for X-ray diffraction were grown from concentrated pentane solution at −35 °C (0.140 g, 0.170 mmol, 86%). ^{1}H NMR (C_7D_8): δ 7.46 (d, 2H, *o*-*H* Ph, $^3J_{H-H}$ = 7.2 Hz), 7.12−6.82 and 6.65 (m, 12H, Ar*H* and *m*,*p*-*H* Ph), 6.06 (s, 1H, C*H*), 5.92 (br s, 1H, N*H*), 3.92 (sp, 2H, $CHMe_2$, $^3J_{H-H}$ = 6.6 Hz), 3.11 (sp, 2H, $CHMe_2$ $^3J_{H-H}$ = 6.7 Hz), 2.06 (sp, 2H, NH-2,6-$(CHMe_2)_2C_6H_3$, $^3J_{H-H}$ = 6.8 Hz), 1.55 (d, 6H, $CHMe_2$, $^3J_{H-H}$ = 6.6 Hz), 1.36 (d, 6H, $CHMe_2$, $^3J_{H-H}$ = 6.6 Hz), 1.19 (d, 6H, $CHMe_2$, $^3J_{H-H}$ = 6.7 Hz), 1.16 (br s, 18H, $NCCMe_3$) 1.09 (d, 6H, $CHMe_2$, $^3J_{H-H}$ = 6.7 Hz), 1.03 (d, 12H, NH-2,6-$(CHMe_2)_2C_6H_3$, $^3J_{H-H}$ = 6.8 Hz). ^{13}C{^{1}H} NMR (C_7D_8): δ 176.46 ($NCCMe_3$), 149.15, 143.63, 142.90, 133.92, 126.86, 126.70, 124.35, 122.91, 118.88, and 117.85 (ArC), 141.70 (ScCC-Ph), 132.08 (*o*-*C* Ph), 128.25 (*m*-*C* Ph), 126.36 (*p*-*C* Ph), 100.83 (ScCCPh), 96.45 (CH), 44.41 ($NCCMe_3$), 32.29 ($NCCMe_3$), 30.73 (NH-2,6-$(CHMe_2)_2C_6H_3$), 29.23 and 28.76 ($CHMe_2$), 27.24, 25.29, 24.58, and 24.47 ($CHMe_2$), 22.75 (NH-2,6-$(CHMe_2)_2C_6H_3$). Anal. Calcd for $C_{60}H_{88}N_3Sc$ (including 1 C_5H_{12} of solvation): C, 80.40; H, 9.90; N, 4.69. Found: C, 79.81; H, 10.57; N, 4.82.

Generation of *d*-*endo*-5. **2** (0.015 g, 0.018 mmol) and *d*-phenylacetylene (2.00 μL, 0.018 mmol) were dissolved in 0.6 mL of d_8-toluene. The solution was mixed thoroughly and heated to 70 °C for 72 h. The ^{1}H NMR spectrum matched that of *endo*-**5**, except that no resonances were observed for the amido proton. ^{2}H NMR (C_7D_8): δ 6.02 (br s, N*D*).

Concentration Dependence of DMAP in the Production of 2·DMAP. In a typical experiment, **3** (0.004 g, 0.005 mmol) and the desired quantity of DMAP were dissolved in 0.5 mL of d_8-toluene at room temperature. The sample was shaken and quickly inserted into the NMR probe. The progress of the reaction was monitored by integration of the amido proton in **3** and the *p*-H of coordinated DMAP in **2**·DMAP in the ^{1}H NMR spectrum. The reaction was followed until 95% completion.

Activation Parameters in the Production of 2·DMAP. In a typical experiment, **3** (0.004 g, 0.005 mmol) and DMAP (0.009 g, 0.074 mmol) were dissolved in 0.5 mL of d_8-toluene at room temperature. The sample was shaken and quickly inserted into the NMR probe, at which time it was given 5 min to equilibrate to the specified temperature. The progress of the reaction was monitored by integration of the amido proton in **3** and the *p*-H of coordinated DMAP in **2**·DMAP in the ^{1}H NMR spectrum. The reaction was followed until 95% completion.

■ ASSOCIATED CONTENT

Ⓢ Supporting Information

CIF files giving crystallographic data for *endo*-**4** and *endo*-**5** and Figures S1−S6, giving the X-ray structure of **3**, additional NMR spectra, and pseudo-first-order plots. This material is available free of charge via the Internet at http://pubs.acs.org.

■ AUTHOR INFORMATION

Corresponding Author

*E-mail: wpiers@ucalgary.ca.

Present Address

†Department of Chemistry, School of Molecular Sciences, La Trobe University, Melbourne, Victoria, Australia.

Author Contributions

The manuscript was written through contributions of all authors. All authors have given approval to the final version of the manuscript.

Notes

The authors declare no competing financial interest.

■ ACKNOWLEDGMENTS

W.E.P. acknowledges the NSERC of Canada for a Discovery Grant and the Canada Council of the Arts for a Killam Research Fellowship (2012−2014).

■ REFERENCES

(1) Cundari, T. R. *Chem. Rev.* **2000**, *100*, 807.
(2) Mountford, P. *Chem. Commun.* **1997**, 2127.
(3) Hazari, N.; Mountford, P. *Acc. Chem. Res.* **2005**, *38*, 839.
(4) Fout, A. R.; Kilgore, U. J.; Mindiola, D. J. *Chem. Eur. J.* **2007**, *13*, 9428.
(5) Gibson, V. C. In *Modern Coordination Chemistry: the Legacy of Joseph Chatt*; Leigh, G. J., Winterton, N., Eds.; Royal Society of Chemistry: London, 2002; p 140.
(6) Schrock, R. R. *Dalton Trans.* **2001**, 2541.
(7) Schrock, R. R. *J. Mol. Catal., A* **2004**, *213*, 21.
(8) Cantrell, G. K.; Meyer, T. Y. *J. Am. Chem. Soc.* **1998**, *120*, 8035.
(9) Walsh, P. J.; Baranger, A. M.; Bergman, R. G. *J. Am. Chem. Soc.* **1992**, *114*, 1708.
(10) Pohlki, F.; Doye, S. *Chem. Soc. Rev.* **2003**, *32*, 104.
(11) Pohlki, F.; Doye, S. *Angew. Chem., Int. Ed.* **2001**, *40*, 2305.
(12) Zhang, Z.; Leitch, D. C.; Lu, M.; Patrick, B. O.; Schafer, L. L. *Chem. Eur. J.* **2007**, *13*, 2012.
(13) Lee, A. V.; Schafer, L. L. *Eur. J. Inorg. Chem.* **2007**, *2007*, 2245.
(14) Walsh, P. J.; Hollander, F. J.; Bergman, R. G. *J. Am. Chem. Soc.* **1988**, *110*, 8729.
(15) Cummins, C. C.; Baxter, S. M.; Wolczanski, P. T. *J. Am. Chem. Soc.* **1988**, *110*, 8731.
(16) Duncan, A. P.; Bergman, R. G. *Chem. Rec.* **2002**, *2*, 431.
(17) Cummins, C. C.; Schaller, C. P.; Van Duyne, G. D.; Wolczanski, P. T.; Chan, A. W. E.; Hoffmann, R. *J. Am. Chem. Soc.* **1991**, *113*, 2985.
(18) Hoyt, H. M.; Michael, F. E.; Bergman, R. G. *J. Am. Chem. Soc.* **2004**, *126*, 1018.
(19) Giesbrecht, G. R.; Gordon, J. C. *Dalton Trans.* **2004**, 2387.
(20) Beetstra, D. J.; Meetsma, A.; Hessen, B.; Teuben, J. H. *Organometallics* **2003**, *22*, 4372.
(21) Gordon, J. C.; Giesbrecht, G. R.; Clark, D. L.; Hay, P. J.; Keogh, D. W.; Poli, R.; Scott, B. L.; Watkin, J. G. *Organometallics* **2002**, *21*, 4726.
(22) Schädle, D.; Schädle, C.; Törnroos, K. W.; Anwander, R. *Organometallics* **2012**, *31*, 5101.
(23) Berthet, J.-C.; Thuéry, P.; Ephritikhine, M. *Eur. J. Inorg. Chem.* **2008**, *2008*, 5455.
(24) Conroy, K. D.; Piers, W. E.; Parvez, M. *Organometallics* **2009**, *28*, 6228.
(25) Scott, J.; Basuli, F.; Fout, A. R.; Huffman, J. C.; Mindiola, D. J. *Angew. Chem., Int. Ed.* **2008**, *47*, 8502.
(26) Knight, L. K.; Piers, W. E.; Fleurat-Lessard, P.; Parvez, M.; McDonald, R. *Organometallics* **2004**, *23*, 2087.
(27) Lu, E.; Li, Y.; Chen, Y. *Chem. Commun.* **2010**, *46*, 4469.
(28) Lu, E. L.; Chu, J. X.; Chen, Y. F.; Borzov, M. V.; Li, G. Y. *Chem. Commun.* **2011**, *47*, 743.
(29) Chu, J.; Lu, E.; Liu, Z.; Chen, Y.; Leng, X.; Song, H. *Angew. Chem., Int. Ed.* **2011**, *50*, 7677.
(30) Basuli, F.; Tomaszewski, J.; Huffman, J. C.; Mindiola, D. J. *Organometallics* **2003**, *22*, 4705.
(31) Hayes, P. G.; Piers, W. E.; Lee, L. W. M.; Knight, L. K.; Parvez, M.; Elsegood, M. R. J.; Clegg, W. *Organometallics* **2001**, *20*, 2533.
(32) Lee, L. W. M.; Piers, W. E.; Elsegood, M. R. J.; Clegg, W.; Parvez, M. *Organometallics* **1999**, *18*, 2947.
(33) Knight, L. K.; Piers, W. E.; McDonald, R. *Organometallics* **2006**, *25*, 3289.
(34) Waterman, R. *Organometallics* **2007**, *26*, 2492.
(35) Roering, A. J.; Leshinski, S. E.; Chan, S. M.; Shalumova, T.; MacMillan, S. N.; Tanski, J. M.; Waterman, R. *Organometallics* **2010**, *29*, 2557.
(36) Johnson, K. R. D.; Hayes, P. G. *Organometallics* **2010**, *30*, 58.
(37) Knight, L. K.; Piers, W. E.; McDonald, R. *Chem. Eur. J.* **2000**, *6*, 4322.
(38) The two coordination sites on scandium are diastereotopic in these complexes, and we have referred to the site "underneath" the C_3N_2 ligand plane as the endo site and that pointing away from the ligand the exo position. These sites are exchangable via a C_{2v} structure in which the Sc atom passes through the ligand plane, but this process is generally slow on the NMR time scale. In dimers, there are three possible isomers depending on the relative orientations of the two scandium centers, and in the slow exchange regime, this is most apparent by observing the region of the spectrum where the nacnac backbone methine hydrogen is found.
(39) Lee, S. Y.; Bergman, R. G. *Tetrahedron* **1995**, *51*, 4255.
(40) Ge, S.; Meetsma, A.; Hessen, B. *Organometallics* **2009**, *28*, 719.
(41) Pangborn, A. B.; Giardello, M. A.; Grubbs, R. H.; Rosen, R. K.; Timmers, F. J. *Organometallics* **1996**, *15*, 1518.
(42) Corrente, A. M.; Chivers, T. *New J. Chem.* **2010**, *34*, 1751.
(43) Berenguer, J. R.; Lalinde, E.; Torroba, J. *Inorg. Chem.* **2007**, *46*, 9919.
(44) Zhou, J.; Hartwig, J. F. *J. Am. Chem. Soc.* **2008**, *130*, 12220.